

## Film Cooling Behavior in Thin Rectangular Channel (Quick Prediction with $k-\epsilon$ Turbulent Model)

M. Osakabe<sup>1</sup>, T. Miyazawa<sup>1</sup>, T. Motoda<sup>1</sup>, Y. W. Wu<sup>1</sup> and K. Nakashima<sup>2</sup>

### ABSTRACT

The present experiment showed that injected jets even from a two-dimensional slit in a thin rectangular channel generated a complex three-dimensional flow, in which flow reversal region existed partially near injection. Quick-prediction method by solving parabolic equations for a low Reynolds number  $k-\epsilon$  model was applied to predict such a complex film cooling behavior in the thin rectangular channel. The separation bubbles just after the injection are considered to be a kind of large eddies in a turbulent duct flow. To simulate the bubbles just after the injection slit, the excess turbulent kinetic energy was superposed to the oncoming  $k$  profile at the injection slit. Predicted film cooling effectiveness were compared with experimental data and showed generally fairly good agreement.

### NOMENCLATURE

$D_h$ : hydraulic diameter  
 $g$ : acceleration due to gravity  
 $H$ : duct height  
 $k$ : turbulent energy  
 $M$ : injection mass flow rate  $[= \rho_2 v_2 / (\rho_1 u_m)]$   
 $P$ : pressure  
 $Pr$ : Prandtl number  
 $Re_1$ : Reynolds number of primary fluid  $(= u_m D_h / \nu_1)$   
 $Re_2$ : Reynolds number of secondary fluid  $(= v_2 s / \nu_2)$   
 $s$ : slit width  
 $T$ : temperature  
 $u$ : velocity in  $x$  direction  
 $v$ : velocity in  $y$  direction  
 $v_2$ : injection velocity  
 $x$ : distance from injection slit  
 $y$ : distance from wall  
 $\epsilon$ : dissipation  
 $\eta_w$ : film cooling effectiveness  $[=(T_w - T_1)/(T_2 - T_1)]$   
 $\mu$ : viscosity  
 $\nu$ : kinematic viscosity  
 $\rho$ : density

subscript

1: primary 2: secondary  $m$ : average in duct cross-section  
 $T$ : turbulent  $W$ : wall

<sup>1</sup> Tokyo University of Mercantile Marine, Tokyo, Japan  
<sup>2</sup> Hiroshima Technical College of Maritime Technology, Hiroshima, Japan

### INTRODUCTION

Thermal efficiency of gas turbines can be improved by increasing the gas temperature. With higher gas temperature a reasonable lifetime of turbine components can be ensured only by protecting them from the hot gas stream. Film cooling is a commonly-used technique for protecting component walls against the hot gas stream. Goldstein[1] summarized the numerous experimental and theoretical studies about the film cooling behavior. However these studies were focused on the film cooling behavior in a low turbulence freestream by using a large wind tunnel. Obata et al.[2] and Sakata et al.[3] pointed out that the film cooling effectiveness is strongly affected with a turbulence level in a mainstream. The actual condition on the turbine components may be very complicated with the strong mainstream turbulence such as in combustion chambers and turbine blades.

One of the critical areas of film cooling for gas turbine is the blade tip region[4]. In axial turbine stages under almost all operating conditions, a clearance gap exists between the blade tips and the stationary outer shroud. In normal operation, the pressure difference between the pressure and suction sides of blades drives a leakage flow through the tip clearance. In these film cooling, it is very difficult to define the mainstream. The previous correlation to predict the film cooling effectiveness was empirically obtained by experiments in a low turbulence mainstream. So an application of the empirical correlation to the narrow flow path should be carefully conducted even if a rough calculation is necessary.

When the flow field is strongly three dimensional, basically a three-dimensional calculation procedure is necessary. Patankar et al.[5] presented such a procedure on the injection from discrete tangential slots. For the three-dimensional calculation of film cooling behavior, numerical grids with 20,000 to 40,000 nodes have been used. With these, converged solutions required between 30 and 90 min of computing time on a large computer system. This time is too long to conduct parameter studies for the optimization of film cooling configuration. For such parameter studies, faster prediction methods are required, such as suitably extended two-dimensional procedures[6].

The present experiment showed that injected jets even from a two-dimensional slit in a thin rectangular channel generated a complex three-dimensional flow, in which flow reversal region existed partially near injection. Quick-prediction method by solving parabolic equations for a low Reynolds number  $k-\epsilon$  model was applied to predict such a complex film cooling behavior. First in this paper, the governing parabolic equations and the turbulence model are given. Then the special modifications are described, which account for the elliptic nature of the flow after the injection such as the partial flow reversal. The predictions are compared with the experimental results obtained in the thin rectangular channel.

**PREVIOUS STUDIES FOR SLIT FILM COOLING**

The slit-flow field is highly complicated for non-tangential injection, and most studies up to the present time has been devoted to experimental studies and semi-empirical models to predict the film cooling effectiveness. The main details of such a flow field for normal injection are shown in Fig.1. Generally the injected flow may separate at the rear of the slit, and subsequently reattach. Downstream of the slit the instability due to the shear layer may increase the turbulent intensity, and mixing of the mainstream and the injected film may occur. For the slit-film cooling effectiveness  $\eta_w$ , Seban et al.[1] proposed the following correlation.

$$\eta_w = 2.2A^{-0.5} \quad (1)$$

where A is non-dimensional parameter which is often used in an analysis of a two-dimensional jet[7] and defined as,

$$A = \frac{x}{Ms} \quad (2)$$

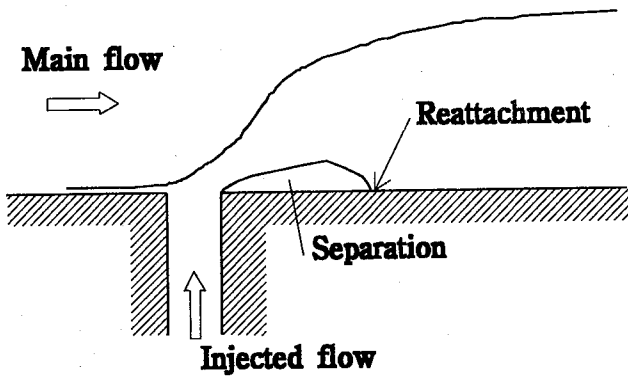


Fig.1 Flow configuration of slit-film cooling

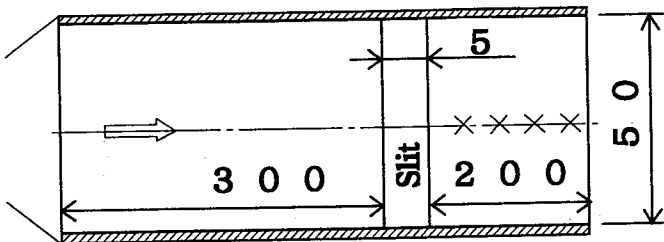
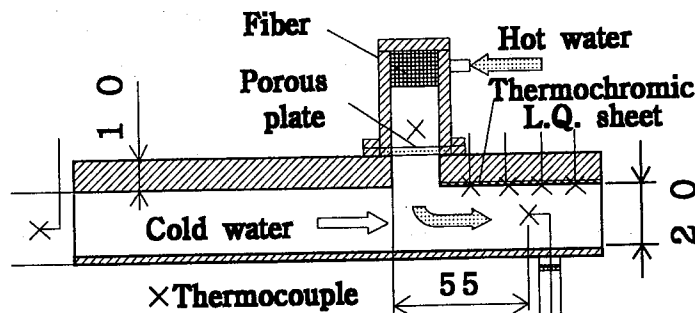


Fig.2 Schematic of test apparatus



where M is a injection mass flow ratio as,

$$M = \frac{\rho_2 V_2}{\rho_1 u_1} \quad (3)$$

where  $u_1$  is a mainstream velocity. In the present study, the average velocity  $u_m$  is used as  $u_1$ . On the other hand, Obata[8] proposed the following correlation by using the same non-dimensional parameter.

$$\begin{aligned} \eta_w &= 1.9A^{-0.45} & 10 \leq A \leq 100 \\ \eta_w &= 9.6A^{-0.8} & 100 \leq A \end{aligned} \quad (4)$$

**EXPERIMENTAL APPARATUS AND MAJOR RESULTS**

Shown in Fig.2 is a schematic of the experimental apparatus[9]. A primary fluid( approximately 20°C cold water) was flowing in the thin rectangular duct and a secondary fluid(approximately 60°C hot water) was injected from the slit of 5 mm width. It was possible to adjust the duct height between 20 and 5 mm to investigate the effect of a narrow space. The flow distribution of the injection was eliminated with the porous plate(mesh 20  $\mu$ ) upstream of the slit. The hot water was supplied from a boiler through a cascade tank where bubbles were separated and removed. The injection slit located at 300 mm(L/D<sub>h</sub> is greater than 10.5) from the duct inlet to ensure a fully turbulent condition in the duct. The test section was made of a transparent acrylic

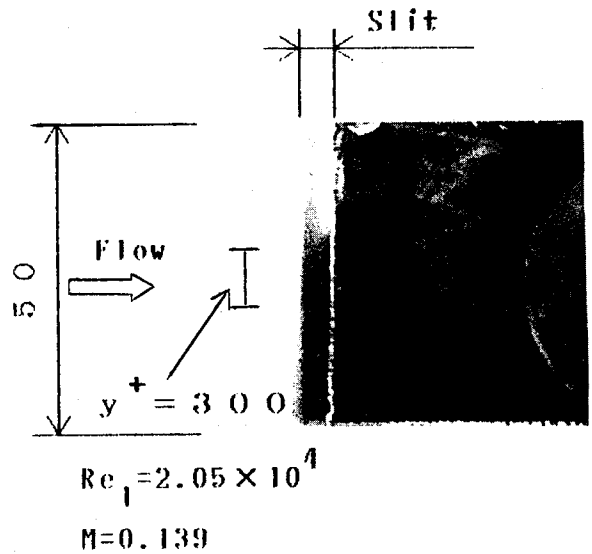


Fig.3 Visualization of wall temperature

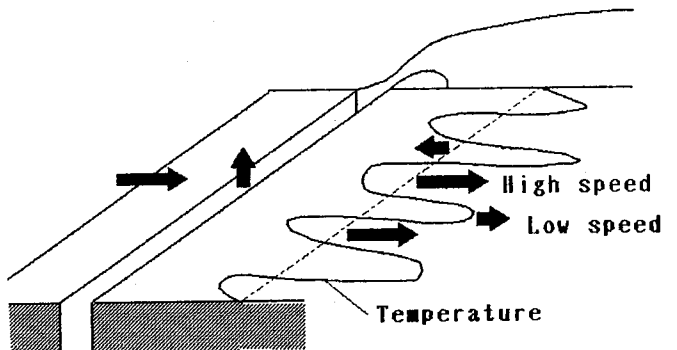


Fig.4 Schematic of observed flow

resin in order to observed the flow behavior. Film thickness and wall temperature distribution were visualized with an ink and a thermochromic liquid crystal sheet, respectively. The wavy temperature distributions on the wall just after the injection slit was observed in spite of two-dimensional film as shown in Fig.3. Hydrogen bubbles generated with a platinum wire near the wall( $y^+ \approx 10$ ) showed the flow configuration as shown in Fig.4. The high speed flow region is corresponding to the low temperature region indicating the invasion of the cold mainstream. At the high temperature region, the low speed flow or the flow reversal was observed.

**LOW REYNOLDS NUMBER TURBULENT MODEL**

No diffusion in the direction of the mainstream and a constant pressure gradient  $dp/dx$  in the duct cross-section were assumed in the present model. It is considered that the latter assumption is adequate to predict the film cooling only at the low injection. For those at the high injection, the special modifications may be necessary, which account for the elliptic nature of the flow after the injection such as the partial flow reversal. However the above assumption enable a quick prediction solving parabolic equations. The parabolic equations are;

$$\frac{\partial u}{\partial x} + \frac{\partial v}{\partial y} = 0 \tag{5}$$

$$\frac{\partial(u^2)}{\partial x} + \frac{\partial(uv)}{\partial y} = \frac{\partial}{\partial y} \left[ (v + v_T) \frac{\partial u}{\partial y} \right] - \frac{1}{\rho} \frac{\partial p}{\partial x} \tag{6}$$

$$\frac{\partial(uk)}{\partial x} + \frac{\partial(vk)}{\partial y} = \frac{\partial}{\partial y} \left[ (v + \frac{v_T}{\sigma_k}) \frac{\partial k}{\partial y} \right] \tag{7}$$

$$+ v_T \left[ \frac{\partial u}{\partial y} \right]^2 - \epsilon - 2v \left[ \frac{\partial k^{1/2}}{\partial y} \right]^2$$

$$\frac{\partial(u\epsilon)}{\partial x} + \frac{\partial(v\epsilon)}{\partial y} = \frac{\partial}{\partial y} \left[ (v + \frac{v_T}{\sigma_\epsilon}) \frac{\partial \epsilon}{\partial y} \right]$$

$$+ C_1 f_1 v_T \left[ \frac{\partial u}{\partial y} \right]^2 \frac{\epsilon}{k} - C_2 f_2 \frac{\epsilon^2}{k} + 2v v_T \left[ \frac{\partial^2 u}{\partial y^2} \right]^2 \tag{8}$$

$$\frac{\partial(uT)}{\partial x} + \frac{\partial(vT)}{\partial y} = \frac{\partial}{\partial y} \left[ (a + \frac{v_T}{Pr_T}) \frac{\partial T}{\partial y} \right] \tag{9}$$

$$v_T = C_\mu f_\mu \frac{k^2}{\epsilon} \tag{10}$$

Several kinds of the constants in the low Reynolds turbulent model has been proposed and Myong et al.[11] summarized the detail. In the present study, the typical constants proposed by Launder-Sharma[12] was used. The constants are  $C_1=1.44$ ,  $f_1=1$ ,  $C_2=1.92$ ,  $Pr_T=0.9$ ,  $\sigma_K=1$ ,  $\sigma_E=1.3$ ,

$$f_2 = 1 - 0.3 \exp(-R_T^2)$$

$$C_\mu = 0.09$$

$$f_\mu = \exp \left[ \frac{-3.4}{(1 + R_T/50)^2} \right]$$

$$R_T = \frac{k^2}{v\epsilon}$$

Shown in Fig.5 is the noding used in the present study. The grid width near the wall is  $y^+=1$  and that is multiplied by 1.1 as far from the wall. The noding is symmetry at the duct center. The boundary conditions at the wall are,

$$u = k = \epsilon = 0$$

and for the wall without the injection,

$$v = 0$$

$$\frac{\partial T}{\partial y} = 0$$

for the wall with the injection,

$$v = v_2$$

$$T = T_2$$

The initial condition just before the injection was the fully turbulent condition calculated with the present model. The difference between the calculation results using the physical value at the temperature of the primary fluid and those at the average temperature of the primary and secondary fluid was negligible. So the physical values at the temperature of the primary fluid was used for the calculation.

In the typical calculation, the number of nodes in the y direction was approximately 85. In x direction, the width of nodes was constant at the slit width. The calculation was conducted by the

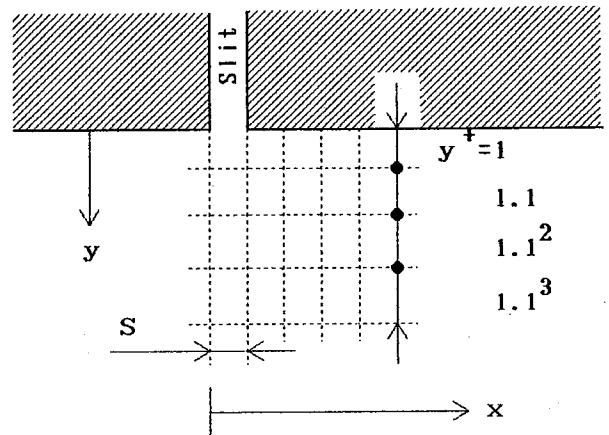


Fig.5 Noding for two-dimensional calculation

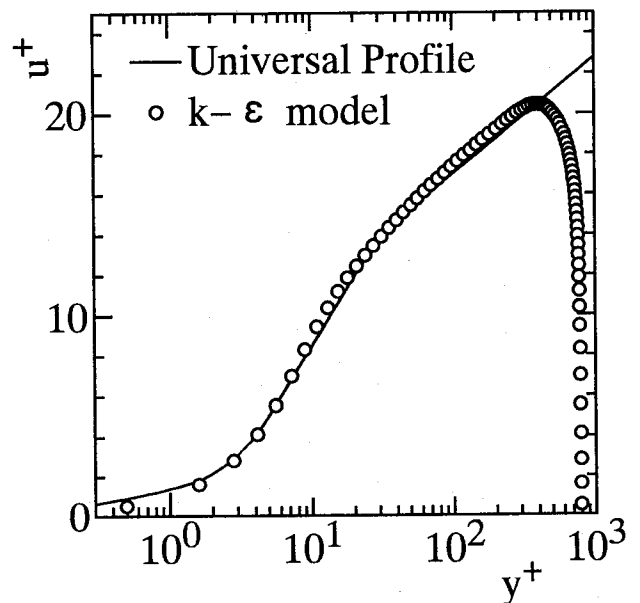


Fig.6 Calculated velocity profiles just before injection slit

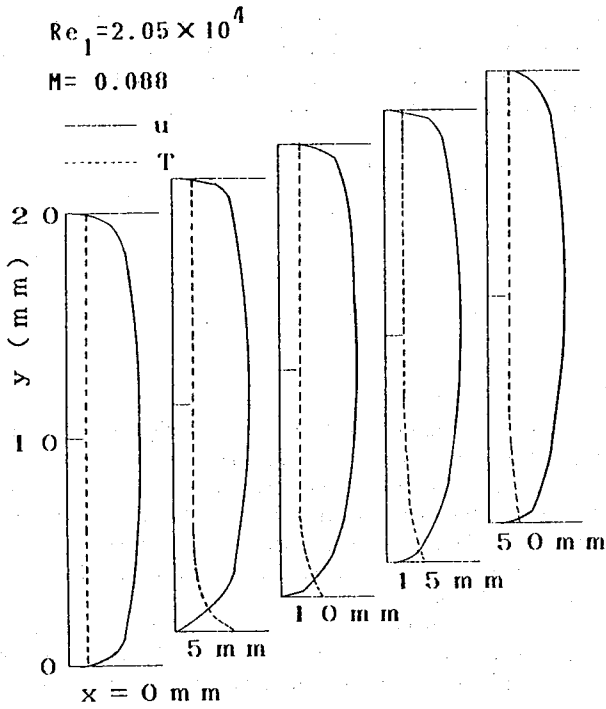


Fig.7 Calculated velocity and temperature profiles

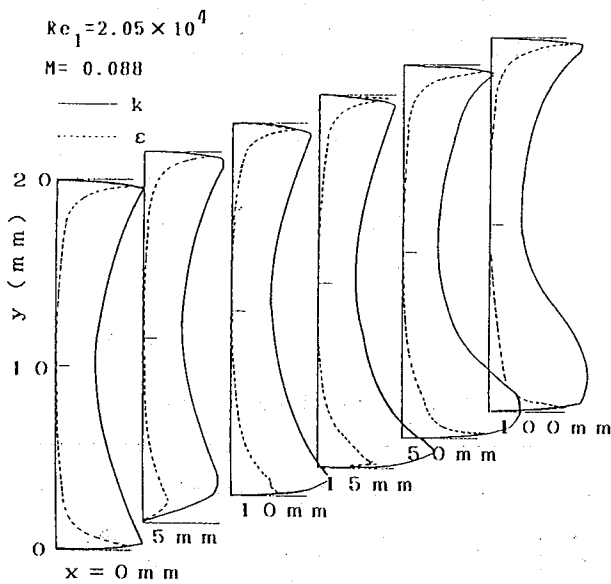


Fig.8 Calculated turbulent energy and dissipation profiles

control-volume method[12] using the first-order up-wind scheme. By using these noding and scheme, the velocity profile at the fully turbulent condition just before the injection agreed well with the universal velocity profile as shown in Fig.6. The converged solutions required only less than 1 min of computing time by using a personal computer(CPU 486DX2).

**CALCULATION RESULTS WITH ORIGINAL MODEL**

Shown in Fig.7 is the typical prediction for the profiles of velocity and fluid temperature. The velocity profile at  $x = 0$  mm corresponds to the fully turbulent duct flow and agrees well with the 1/8 power law profile. At the node of  $x = 5$  mm, the velocity profile is shifted up due to the injected hot water and the hot water film layer is generated near the wall. Downstream of the

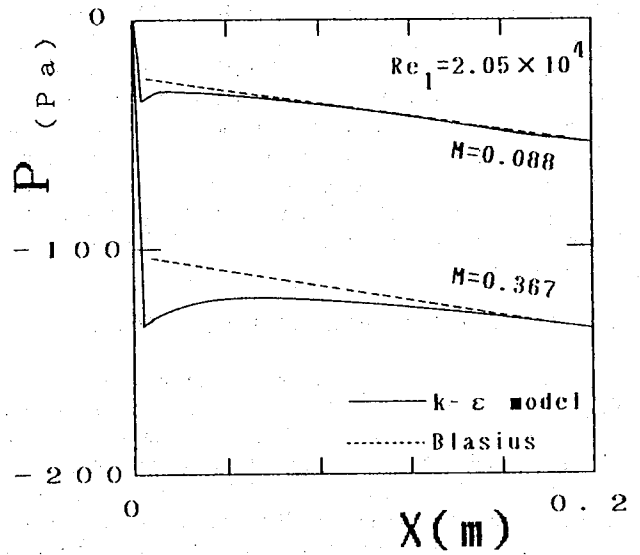


Fig.9 Calculated pressure curves

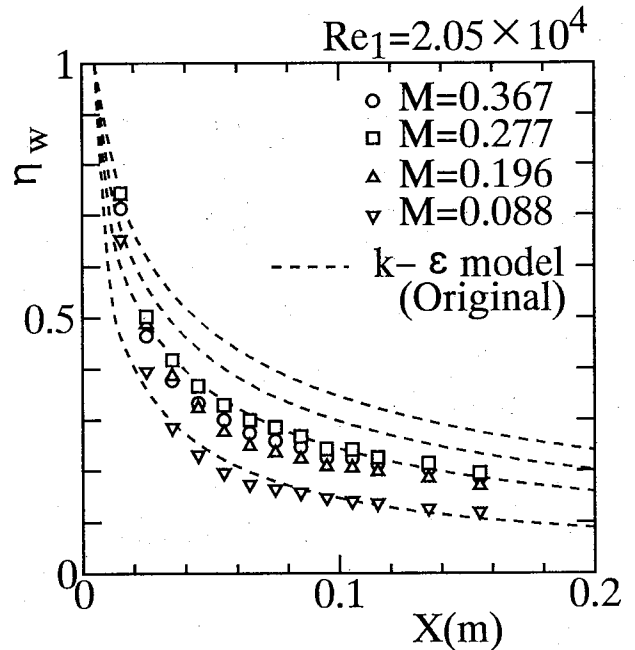


Fig.10 Calculation results with original model

injection slit, the velocity profile descends again to the wall and the diffusion of hot water takes place.

Shown in Fig.8 are profiles of  $k$  and  $\epsilon$  at the same calculation conditions as Fig.7. Typical saddle-like profiles indicating a fully turbulent duct flow can be observed at  $x = 0$  mm. At the injection node at  $x = 5$  mm, the  $k$  profile is shifted up and the dissipation  $\epsilon$  is depressed near the wall. Because the  $k$  and  $\epsilon$  of the injected secondary fluid are assumed as zero. Downstream of the injection slit, the  $k$  profile descends again to the wall and the dissipation  $\epsilon$  is increased suggesting the enhancement of heat and mass transfer at the wall.

Shown in Fig.9 is pressure distributions in  $x$  direction at the different mass flow rate  $M$ . The broken lines show the pressure curve calculated with the Blasius friction factor. At the injection slit, the larger undershoot of pressure as the larger mass flow rate  $M$  can be observed. Far from the injection slit, the pressure curves by the model agrees well with that by the Blasius factor. The

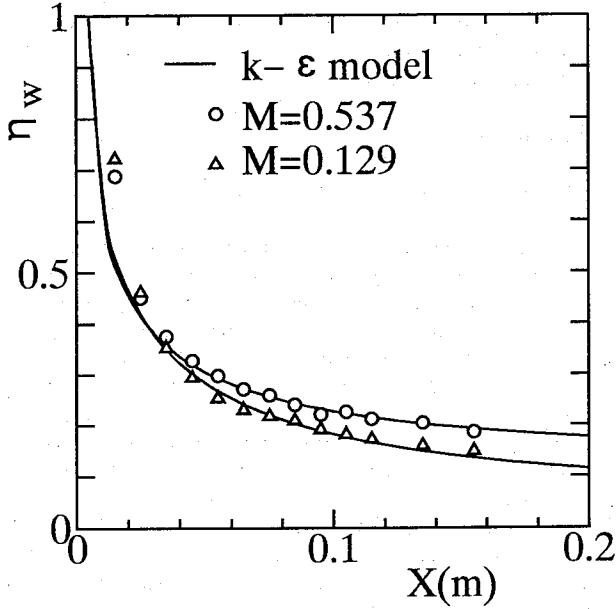


Fig.11 Calculated results with modified model at  $Re_1 = 1.4 \times 10^4$

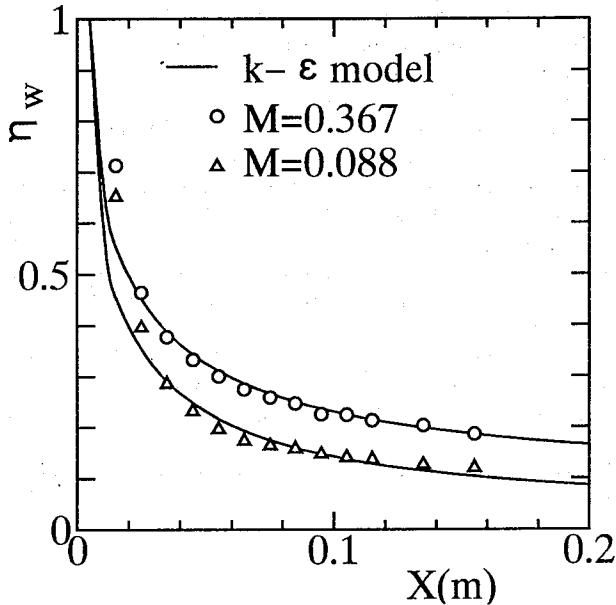


Fig.12 Calculated results with modified model at  $Re_1 = 2.05 \times 10^4$

inverse pressure gradient just after the injection slit suggests the elliptic nature of flow.

Shown in Fig.10 are film cooling effectiveness at the different mass flow rate  $M$ . At the low injection case of  $M=0.088$ , the model prediction agrees well with the experimental results. The film cooling effectiveness by the model monotonously increases with the mass flow rate. However, the experimental effectiveness has a maximum approximately at  $M=0.277$ .

**CALCULATION RESULTS WITH MODIFIED MODEL**

The original model using parabolic equations failed to predict the limitation of the film cooling effectiveness in the thin rectangular channel. Then the special modifications were

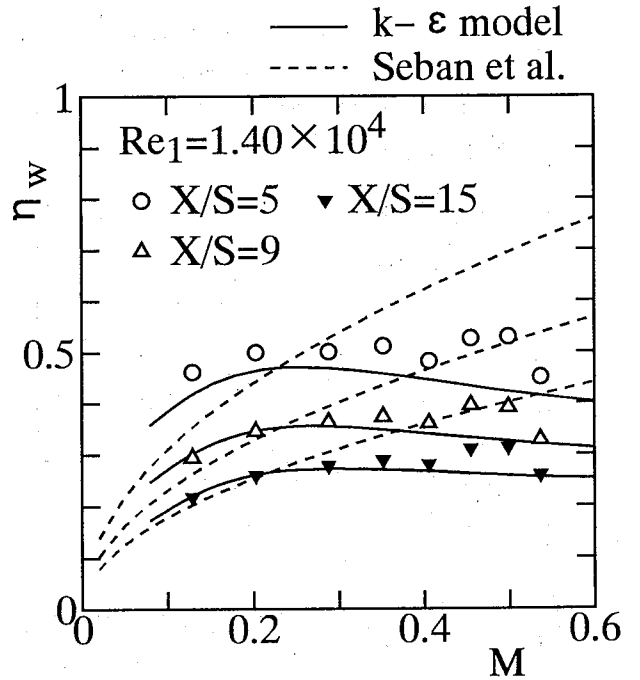


Fig.13 Relation of film cooling effectiveness and mass flow ratio at  $Re_1 = 1.4 \times 10^4$

considered, which account for the elliptic nature of the flow after the injection such as the partial flow reversal. It is impossible to simulate the complicated region of the separation bubbles with the two-dimensional parabolic equations. So the separation bubbles are considered to be a kind of large eddies in a turbulent duct flow. To simulate the bubbles just after the injection slit, the excess turbulent kinetic energy was superposed to the oncoming  $k$  profile at  $x=0$  mm. The excess  $k$  profile was approximated by a parabolic distribution as ,

$$k = (\beta v_2)^2 \sin(\pi y / H) \tag{11}$$

where  $\beta=0.27$  is used in the present study. Using the superposed  $k$  distribution, the profile for the dissipation rate  $\epsilon$  is finally determined.

Predicted film cooling effectiveness are compared with experimental data and show generally fairly good agreement as shown in Figs.11 and 12 at the different mass flow rate  $M$  and the primary Reynolds number. Shown in Figs.13 and 14 are the relation of the cooling effectiveness and the mass flow rate  $M$ . The broken lines are calculated with the empirical correlation by Seban et al.. The correlation shows the higher cooling effectiveness as the larger mass flow rate  $M$ . However, the experimental data tends to have a maximum at a certain value of  $M$ . The modified model predicts well the experimental tendency.

**CONCLUSION**

Film cooling behavior in thin rectangular channel was studied experimentally by using water and the quick-prediction method was proposed. The following major results were obtained.

- (1) The wavy temperature distributions on the wall just after the injection slit was observed in spite of two-dimensional film. The high speed flow region near the wall is corresponding to the low temperature region indicating the invasion of the cold mainstream. At the high temperature region, the low speed flow or the flow reversal was observed.

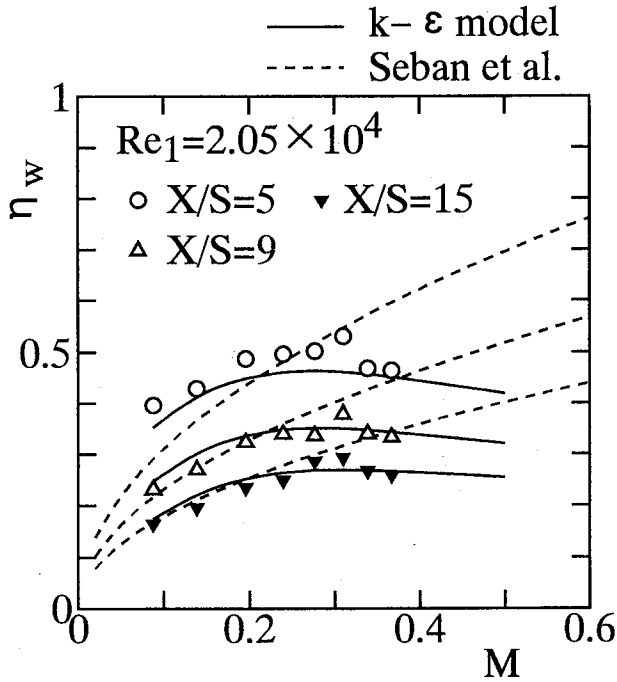


Fig. 14 Relation of film cooling effectiveness and mass flow ratio at  $Re_1 = 2.05 \times 10^4$

(2) Quick-prediction method by solving the parabolic equations for a low Reynolds number  $k-\epsilon$  model was applied to predict such a complex film cooling behavior in the thin rectangular channel. At the low injection case, the model prediction for the film cooling effectiveness agreed well with the experimental results. The cooling effectiveness by the model monotonously increased with the mass flow rate. However, the experimental effectiveness had a maximum at a certain value of  $M$ .

(3) The original model using the parabolic equations failed to predict the limitation of the film cooling effectiveness in the thin rectangular channel. Then the special modifications were considered, which account for the elliptic nature of the flow after the injection such as the partial flow reversal. It is impossible to simulate the complicated region of the separation with the parabolic equations. The separation bubbles are considered to be a kind of large eddies in a turbulent duct flow. To simulate the

bubbles just after the injection slit, the excess turbulent kinetic energy was superposed to the oncoming  $k$  profile at the injection slit. Predicted film cooling effectiveness were compared with experimental data and showed generally fairly good agreement.

#### REFERENCES

- [1] Goldstein, R.J., "Advances in heat transfer", Vol.7, Academic Press, 1971, 321-377
- [2] Obata, M. and Hirata, Y., "Effect of mainstream turbulence on film cooling", (in Japanese), Proc. of JSME, 770-8, 1977, 145-147
- [3] Sakata, K. and Shindo, S., "Turbulence effect on mixing of film-cooling flow tested with water flow model", Proc. of Yokohama Int. Gas Turbine Conference, 1991, II 201-214
- [4] Kim, Y.W., Abdel-Messeh, W., Downs, J.P., Sechting, F.O., Steuber, G.D. and Tanrikut, S., "A summary of the cooled turbine blade tip heat transfer and film effectiveness investigations performed by Dr.D.E.Metzger", ASME paper 94-GT-167, 1994
- [5] Patankar, S.V., Rastogi, A.K. and Whitelaw, J.H., "The effectiveness of three-dimensional film-cooling slots - II Predictions", Int. J. Heat and Mass Transfer, 16, 1973, 1665-1681
- [6] Schonung, B. and Rodi, R., "Prediction of film cooling by a row of holes with a two-dimensional boundary-layer procedure", J. of Turbomachinery, 109, 1987, 579-587
- [7] Humber, A.J., Grandmaison, E.W. and Pollard, A., "Mixing between a sharp-edged rectangular jet and a transverse cross flow", Int. J. Heat Mass Transfer, 36(18), 1993, 4307-4316
- [8] Obata, M., "Experimental study for slit film cooling with large injection angle", (in Japanese), Proc. of JSME, No.710-14, 1971, 213-216
- [9] Osakabe, M., Miyazawa, T., Horiki, S., Mikawa, D. and Obata, M., "Film cooling in thin rectangular channel -Comparison of experimental results with previous correlation and  $k-\epsilon$  model", (in Japanese), J. of MESJ, 30(5), 1995, 397-404
- [10] Myong, H.K. and Kasagi, N., "A new proposal for a  $k-\epsilon$  turbulence model and its evaluation( 1st report, development of the model)", (in Japanese), Trans. of JSME, B54(507), 1988, 3003-3009
- [11] Launder, B.E. and Sharma, B.I., "Application of the energy dissipation model of turbulence to the calculation of flow near a spinning disk", Letters in Heat and Mass Transfer, 1, 1974, 131-138
- [12] Patankar, S.V., Numerical Heat Transfer and Fluid Flow, McGraw-Hill, (1980)